JOURNAL OF CHEMICAL & ENGINEERING DATA

Article

pubs.acs.org/jced

Density of Water (1) + Monoethanolamine (2) + CO_2 (3) from (298.15 to 413.15) K and Surface Tension of Water (1) + Monoethanolamine (2) from (303.15 to 333.15) K

Jingyi Han,[†,‡] Jing Jin,[‡] Dag A. Eimer,[†,‡] and Morten C. Melaaen*[,†,‡]

[†]Tel-Tek, 3918 Porsgrunn, Norway

[‡]Telemark University College, 3901 Porsgrunn, Norway

ABSTRACT: Densities in liquid solutions of monoethanolamine (MEA) and water have been measured at temperatures from (298.15 to 423.15) K. The mass fraction of MEA ranged from 0.3 to 1.0. Excess volumes were correlated by a Redlich−Kister equation. The model uses a third-order Redlich−Kister equation and a linear relationship with the temperature. Densities of CO_2 loaded aqueous MEA solutions were measured at temperatures from (298.15 to 413.15) K. The mass fraction of MEA was 0.3, 0.4, 0.5, and 0.6. Molar volumes of CO_2 loaded aqueous MEA solutions were correlated by the equations from the literature. Polynomial equations are in turn used to correlate the parameters with the temperature. Surface tensions of aqueous MEA solutions were measured at temperatures from (303.15 to 333.15) K. The mass fraction of MEA ranged from 0 to 1.0. The experimental surface tension data were correlated with temperature and mole fraction, respectively.

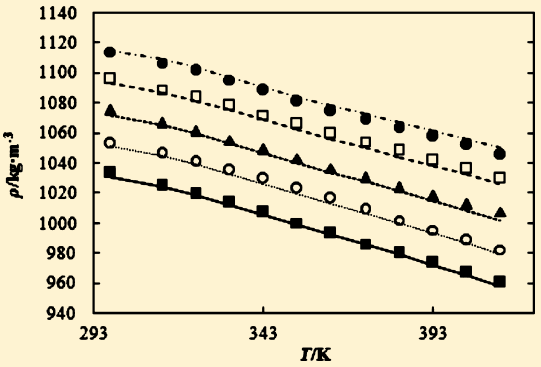

INTRODUCTION

Monoethanolamine (MEA) has been used for the absorption of acid gases since 1930. The mass fraction of MEA was generally increased from 0.15 to 0.30 by 1970, and this has been standard since then although higher compositions have been explored on a research basis. Recent attention given to CO_2 capture from exhaust gases to avoid global warming has caused increased interest in MEA due to its high affinity for CO_2. Very large absorbent flows would need to be circulated. A further increase in mass fraction of MEA would help to reduce these flows. Densities and surface tensions of these solutions are needed to perform a variety of engineering calculations.

Density data for aqueous MEA solutions have previously been reported by a number of authors. These are summarized in Table 1 where ranges of concentrations and temperatures investigated are given for each source. There is also information on the number of points measured and the method used by all authors. Apart from those works summarized in Table 1, it is known that Weiland et al.[11] refer to unpublished data transmitted to the Gas Processors Association in 1993. These data have not been accessed here. Literature values cover the entire composition range up to 353.15 K.

In the present work densities of unloaded aqueous MEA solutions with mass fractions of MEA from 0.3 to 1.0 were measured from (298.15 to 423.15) K. This temperature range also covers data needed for engineering estimates related to the desorption part of the CO_2 capture process which previous investigations did not include. These measurements also represent a concerted effort to cover densities for the full range of temperatures and compositions normally met when performing process engineering design estimates.

Densities of CO_2-loaded aqueous MEA solutions are also important. However, little literature can be found. Weiland et al.[11] measured the densities of CO_2-loaded aqueous MEA solutions with mass fractions of MEA from 0.1 to 0.4 at 298.15 K using hydrometers. Amundsen et al.[14] measured the densities of CO_2-loaded aqueous MEA solutions with mass fractions of MEA from 0.2 to 0.4 at (298.15 to 353.15) K using an Anton Paar density meter (DMA 4500) which has high accuracy in wide temperature ranges. The objective of the present work was to measure the densities of CO_2-loaded aqueous MEA solutions with mass fractions of MEA in the (MEA + water) solutions from 0.3 to 0.6 at (298.15 to 413.15) K.

Vázquez et al.[15] measured the surface tensions of aqueous MEA solutions with mass fractions of MEA from 0 to 1.0 at (298.15 to 323.15) K using the Wilhelmy plate principle. In the present work the surface tensions of aqueous MEA solutions were measured with mass fractions of MEA from 0 to 1.0 at (303.15 to 333.15) K using the pendant drop method.

EXPERIMENTAL SECTION

Sample descriptions of MEA and CO_2 are given in Table 2. Aqueous MEA solutions were prepared with water which was produced by a Milli-Q integral water purification system (18.2 MΩ cm). MEA and Milli-Q water were degassed by a rotary evaporator before mixing. All samples (of approximately 0.5 kg)

Received: October 17, 2011
Accepted: February 17, 2012
Published: March 6, 2012

Table 1. Reported Liquid Density Measurements of Water (1) + MEA (2)

source	w_2		T/K		number of measurements	method[a]
	low	high	low	high		
Leibush and Shorina[1] (1947)	0.2	1.0	283.15	353.15	40	Pyc
Touhara et al.[2] (1982)	0	1.0	298.15	298.15	14	Pyc
Murrieta-Guevara and Rodriguez[3] (1984)	1.0	1.0	298.15	333.15	8	Sod
Wang et al.[4] (1984)	1.0	1.0	293.15	361.15	5	Pyc
Li and Shen[5] (1992)	0.3	1.0	303.15	353.15	16	Pyc
DiGullio et al.[6] (1992)	1.0	1.0	294.15	431.15	8	Pyc
Pagé et al.[7] (1993)	0	1.0	283.15	313.15	69	Sod
Maham et al.[8] (1994)	0	1.0	298.15	353.15	110	AP
Li and Lie[9] (1994)	0.2	1.0	303.15	353.15	12	Pyc
Lee and Lin[10] (1995)	0.27	1.0	303.15	323.15	30	Pyc
Weiland et al.[11] (1998)	0.1	0.4	298.15	298.15	4	Hyd
Mandal et al.[12] (2003)	0.3	0.3	293.15	323.15	7	Pyc
Pouryosefi and Idem[13] (2008)	0	1.0	295.15	333.15	88	AP
Amundsen et al.[14] (2009)	0.2	1.0	298.15	353.15	35	AP
present work	0.3	1.0	298.15	423.15	160	AP

[a]AP: Anton Paar (oscillating)/Hyd: hydrometer/Pyc: pycnometer/Sod: Sodev (oscillating).

Table 2. Chemical Sample Descriptions

chemical name	source	initial mole fraction purity	purification method	analysis method
MEA[a]	Merck	0.995	none	GC[b]
carbon dioxide	AGA	0.9999	none	

[a]Monoethanolamine. [b]Gas−liquid chromatography.

were prepared using an analytical balance with an accuracy of $\pm$ 1·10^{-7} kg.

CO_2-loaded aqueous MEA solutions were prepared by bubbling CO_2 through an unloaded solution at the rate 0.150 NL·min^{-1}. The resulting high loaded aqueous MEA solutions were analyzed by a method based on the precipitation of $BaCO_3$ and titration. A sample of (0.05 to 0.1) g was mixed together with 41.7 mL of 0.3 M $BaCl_2$ solution and 50 mL of 0.1 M NaOH solution. This mixture was boiled for (4 to 5) min, cooled down in a bath, and then filtrated. The filter cake was added to 50 mL of degassed, distilled water and then titrated with 0.1 M HCl solution to pH 2. The mixture was finally titrated with NaOH to pH 5.27 to calculate the amount of excess HCl. Unloaded and high loaded aqueous solutions were then mixed to produce a set of samples with a range of CO_2-loadings.

Densities of unloaded and loaded aqueous MEA solutions were measured using an Anton Paar density meter (DMA 4500) in the temperature range (298.15 to 363.15) K. The instrument was calibrated using air and water. The DMA 4500 is limited to measurements up 363.15 K.

Densities of unloaded and loaded aqueous MEA solutions were measured using an Anton Paar density meter (DMA HP) in the temperature range (373.15 to 423.15) K. DMA HP can be used when the temperature is higher than 363.15 K because the pressure in U-tube is high which can restrain the evaporation of MEA and CO_2 through desorption. This instrument must be calibrated every time before it is used while the calibration of the 4500 model may be done a little less frequently. Nitrogen and water were used for calibration. Both densimeters are based on an oscillating U-tube technique to determine densities.

Surface tension was measured at 10 K intervals, from (303.15 to 333.15) K using a Rame-Hart model 500 Advanced Goniometer with DROPimage Advanced v2.4, which employs the pendant drop method. The surface tension is calculated by use of the droplet geometry size which is obtained by digitizing the image from the camera. The traditional method that measures a liquid droplet has not been adopted because the concentration of component in the droplet changes due to evaporation when the temperature is rising. In addition, the temperature of small droplet is not easy to monitor and control. A bubble was measured instead. A cuvette was used to contain liquid and make sure the light did not change directions. The way to generate the bubble is by first sucking the liquid from the cuvette to the needle by a dispenser, and then sucking the gas into the needle, and finally pushing the liquid and gas from the needle to the cuvette. The values of the mole fractions of MEA, x_2, correspond to the mass fractions from 0 to 1.0, at 0.1 intervals as shown in Table 8. Each surface tension value reported was an average of 10 measurements, where the maximum deviations from the average value were less than 0.0004 N·m^{-1}.

RESULTS AND DISCUSSION

All of the density measurements and the deduced excess volumes of water (1) + MEA (2) solutions are given in Table 3. Densities of pure water are from the International Association for the Properties of Water and Steam (IAPWS). The temperature ranges from (298.15 to 423.15) K, and the composition ranges from w_2 = 0 to 1.0. The pressure was atmospheric below 373.15 K and 0.7 MPa from 373.15 K and higher.

Figure 1 displays the densities of aqueous MEA solutions for selected temperatures as a function of composition. The maximum value on each curve always occurs at w_2 = 0.5 to 0.7. The densities become lower when the temperature increases for all of the compositions. Pure MEA densities may be higher or lower than that of water depending on the temperature.

Figure 2 shows the excess molar volume trends of aqueous MEA solutions for selected temperatures. The behavior with respect to composition is the same over the whole temperature range. It may be noted that the excess molar volumes of water (1) + MEA (2) solutions were less negative when the temperature was increased and that this trend is the same at the higher pressure used in the range (373.15 to 423.15) K.

Table 3. Mass Fraction w, Liquid Densities ρ/kg·m^{-3}, and Deduced Excess Molar Volume V_m^E/m^3·mol^{-1} for the [Water (1) + MEA (2)] Mixture[a,b,c,d]

		298.15 K		303.15 K		308.15 K		313.15 K		318.15 K		323.15 K		328.15 K	
w_2	x_2	ρ	$10^6\ V_m^E$	ρ	$10^6\ V_m^E$	ρ	$10^6\ V_m^E$	ρ	$10^6\ V_m^E$	ρ	$10^6\ V_m^E$	ρ	$10^6\ V_m^E$	ρ	$10^6\ V_m^E$
0	0	997.0	0	995.6	0	994.0	0	992.2	0	990.2	0	988.0	0	985.7	0
0.3	0.1122	1010.9	−0.213	1008.4	−0.205	1006.2	−0.210	1003.5	−0.205	1001.1	−0.211	998.1	−0.206	995.5	−0.213
0.4	0.1643	1016.3	−0.330	1013.8	−0.328	1011.0	−0.323	1008.3	−0.324	1005.3	−0.321	1002.3	−0.322	999.2	−0.320
0.5	0.2278	1021.3	−0.457	1018.2	−0.445	1015.2	−0.446	1012.1	−0.442	1009.0	−0.441	1005.6	−0.437	1002.4	−0.437
0.6	0.3067	1024.8	−0.572	1021.4	−0.562	1018.2	−0.559	1014.7	−0.552	1011.4	−0.550	1007.8	−0.545	1004.4	−0.545
0.7	0.4077	1026.3	−0.651	1022.8	−0.644	1019.3	−0.638	1015.7	−0.633	1012.0	−0.629	1008.3	−0.624	1004.6	−0.622
0.8	0.5412	1024.7	−0.632	1021.0	−0.626	1017.3	−0.622	1013.5	−0.617	1009.7	−0.612	1005.9	−0.610	1002.0	−0.606
0.9	0.7264	1020.0	−0.461	1016.2	−0.459	1012.3	−0.454	1008.5	−0.454	1004.5	−0.449	1000.6	−0.450	996.7	−0.447
1.0	1	1011.9	0	1008.0	0	1004.0	0	1000.0	0	996.0	0	992.0	0	988.0	0
		333.15 K		338.15 K		343.15 K		348.15 K		353.15 K		358.15 K		363.15 K	
w_2	x_2	ρ	$10^6\ V_m^E$	ρ	$10^6\ V_m^E$	ρ	$10^6\ V_m^E$	ρ	$10^6\ V_m^E$	ρ	$10^6\ V_m^E$	ρ	$10^6\ V_m^E$	ρ	$10^6\ V_m^E$
0	0	983.2	0	980.5	0	977.7	0	974.8	0	971.8	0	968.6	0	965.3	0
0.3	0.1122	992.3	−0.208	989.5	−0.215	986.1	−0.211	983.0	−0.218	979.4	−0.214	976.1	−0.220	972.5	−0.221
0.4	0.1643	996.1	−0.322	992.7	−0.321	989.4	−0.323	985.9	−0.323	982.4	−0.324	978.7	−0.325	975.0	−0.326
0.5	0.2278	999.0	−0.437	995.4	−0.435	991.9	−0.435	988.3	−0.435	984.5	−0.434	980.8	−0.435	976.9	−0.435
0.6	0.3067	1000.7	−0.540	997.1	−0.541	993.2	−0.537	989.5	−0.538	985.6	−0.535	981.8	−0.537	977.7	−0.533
0.7	0.4077	1000.8	−0.619	997.0	−0.618	993.1	−0.614	989.2	−0.614	985.2	−0.610	981.2	−0.610	977.1	−0.609
0.8	0.5412	998.2	−0.605	994.2	−0.602	990.2	−0.602	986.2	−0.599	982.1	−0.598	978.0	−0.595	973.9	−0.595
0.9	0.7264	992.7	−0.447	988.7	−0.445	984.6	−0.445	980.6	−0.446	976.5	−0.445	972.3	−0.442	968.1	−0.444
1.0	1	983.9	0	979.8	0	975.8	0	971.6	0	967.5	0	963.4	0	959.2	0
		373.15 K		383.15 K		393.15 K		403.15 K		413.15 K		423.15 K			
w_2	x_2	ρ	$10^6\ V_m^E$	ρ	$10^6\ V_m^E$	ρ	$10^6\ V_m^E$	ρ	$10^6\ V_m^E$	ρ	$10^6\ V_m^E$	ρ	$10^6\ V_m^E$		
0	0	958.6	0	951.2	0	943.4	0	935.1	0	926.3	0	917.1	0		
0.3	0.1122	965.3	−0.224	957.4	−0.223	949.1	−0.224	940.6	−0.227	931.7	−0.229	922.3	−0.227		
0.4	0.1643	967.2	−0.319	959.1	−0.317	950.7	−0.316	941.9	−0.317	932.9	−0.317	923.3	−0.311		
0.5	0.2278	969.0	−0.428	960.6	−0.424	952.0	−0.422	943.1	−0.421	934.0	−0.420	924.3	−0.416		
0.6	0.3067	969.4	−0.522	960.8	−0.516	952.1	−0.513	943.1	−0.509	933.8	−0.506	924.1	−0.497		
0.7	0.4077	968.5	−0.592	959.8	−0.583	950.9	−0.578	941.9	−0.574	932.6	−0.570	922.8	−0.559		
0.8	0.5412	965.3	−0.579	956.5	−0.572	947.6	−0.567	938.6	−0.562	929.3	−0.557	919.5	−0.546		
0.9	0.7264	959.3	−0.413	950.6	−0.409	941.7	−0.405	932.7	−0.403	923.6	−0.401	914.1	−0.393		
1.0	1	950.9	0	942.3	0	933.5	0	924.7	0	915.7	0	906.4	0		

[a]The data were measured under 0.1 MPa from (298.15 to 363.15) K and under 0.7 MPa from (373.15 to 423.15) K. [b]Pure water data are from IAPWS.[16] [c]Excess molar volumes of aqueous MEA solutions here are derived data. [d]The uncertainties are given in Table 12.

dx.doi.org/10.1021/je2010038 | J. Chem. Eng. Data 2012, 57, 1095−1103

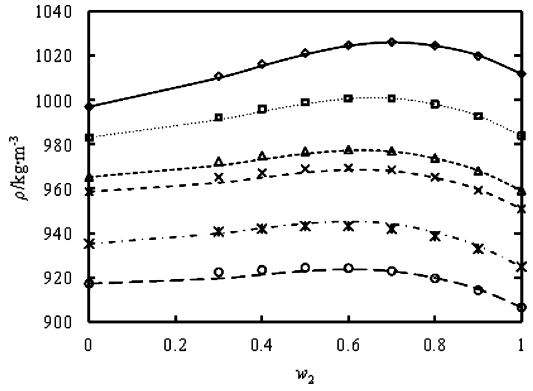

Figure 1. Densities of the H_2O (1) + MEA (2) solutions at selected temperatures. Symbols refer to experimental data: ◊, 298.15 K; □, 333.15 K; △, 363.15 K; ×, 373.15 K; ∗, 403.15 K; ○, 423.15 K. Lines are correlated data: —, 298.15 K; ···, 333.15 K; ---, 363.15 K; ——, 373.15 K; ·-·-, 403.15 K; ———, 423.15 K.

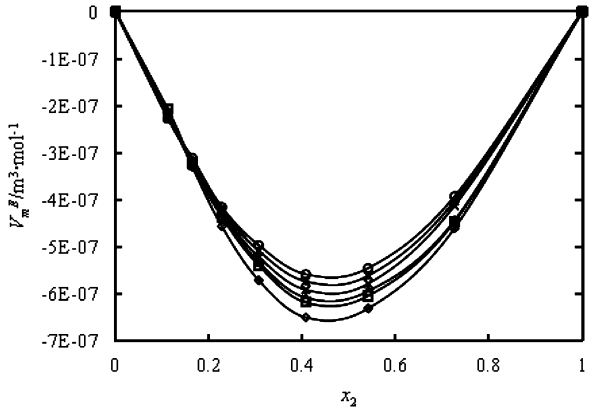

Figure 2. Excess molar volumes of H_2O (1) + MEA (2) solutions at selected temperatures: ◊, 298.15 K; □, 333.15 K; △, 363.15 K; ×, 373.15 K; ∗, 403.15 K; ○, 423.15 K.

There is no marked discontinuity when the measurements are shifted from one densimeter to the other as evidenced by the curves shown in Figure 3.

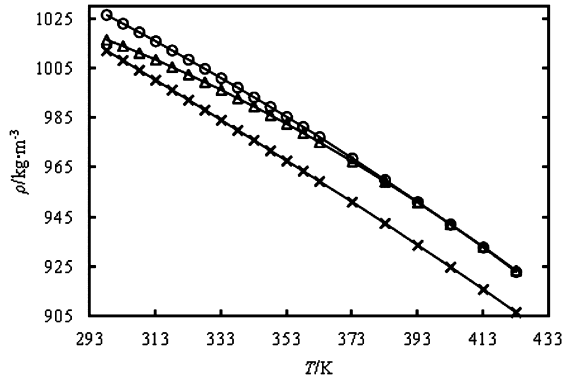

Figure 3. Densities of H_2O (1) + MEA (2) solutions at selected mass fractions of MEA: △, 0.4; ○, 0.7; ×, 1.0.

Densities of CO_2-loaded aqueous MEA solutions are tabulated in Tables 4 to 7 for various mass fractions of MEA. The variations of densities of CO_2-loaded aqueous MEA solutions with temperature and CO_2 loading at a mass fraction of MEA in (water + MEA) solutions equal to 0.3 are shown in Figure 4. As can be seen from the figure, densities of CO_2 loaded aqueous MEA solutions decrease with temperature rising and increase with CO_2 loading rising. Figure 5 shows the densities as a function of CO_2 loading at 323.15 K and mass fractions of MEA in (water + MEA) solutions from 0.3 to 0.5. The densities increase faster with CO_2 loading when the concentration of MEA is higher.

A comparison of measured densities for w_2 = 0.3, 0.4, and 0.5 unloaded aqueous MEA solutions between this work and available literature values[13] is shown in Figure 6. Measurements from this work were on average 0.19 kg·m^{-3} higher for w_2 = 0.3, 0.33 kg·m^{-3} higher for w_2 = 0.4, and 0.30 kg·m^{-3} higher for w_2 = 0.5, respectively, when compared to the values from Pouryosefi and Idem. Measured densities of CO_2-loaded aqueous MEA solutions are compared with literature values at 298.15 K in Figure 7. The maximum deviation between this work and the data from Weiland et al.[11] is 12 kg·m^{-3}. These deviations in results are within the acceptable error.

Table 4. Liquid Densities ρ for Water (1) + MEA (2) + CO_2 (3) from T = (298.15 to 413.15) K and CO_2 Loadings from α = (0.10 to 0.56) n_{CO_2}/n_{MEA} at w_2 = 0.3[a,b]

		α				
T/K	p/MPa	0.10	0.21	0.32	0.44	0.56
		ρ/kg·m^{-3}				
298.15	0.1	1033.3	1053.4	1075.6	1096.4	1114.2
313.15	0.1	1025.3	1046.4	1066.9	1089.1	1106.8
323.15	0.1	1019.6	1041.2	1061.3	1083.8	1101.4
333.15	0.1	1013.8	1035.6	1055.6	1078.2	1095.7
343.15	0.1	1007.6	1029.7	1049.6	1072.3	1088.7
353.15	0.1	1000.2	1023.4	1043.4	1066.0	1081.2
363.15	0.1	993.6	1016.7	1036.7	1059.5	1074.9
373.15	0.7	986.5	1009.2	1030.6	1054.5	1069.1
383.15	0.7	980.1	1002.3	1024.2	1048.2	1063.3
393.15	0.7	973.7	995.7	1018.3	1041.7	1057.6
403.15	0.7	967.4	988.9	1012.9	1036.1	1051.9
413.15	0.7	960.5	982.6	1007.9	1029.5	1045.6

[a] w_2 is the mass fraction of MEA in the (water + MEA) solutions. [b] The uncertainties are given in Table 12.

Table 5. Liquid Densities ρ for Water (1) + MEA (2) + CO_2 (3) from T = (298.15 to 413.15) K and CO_2 Loadings from α = (0.10 to 0.45) n_{CO_2}/n_{MEA} at w_2 = 0.4[a,b]

		α			
T/K	p/MPa	0.10	0.21	0.33	0.45
		ρ/kg·m^{-3}			
298.15	0.1	1037.6	1062.7	1094.5	1129.6
313.15	0.1	1029.5	1054.7	1086.7	1119.9
323.15	0.1	1023.7	1049.0	1081.1	1113.8
333.15	0.1	1017.8	1043.0	1075.2	1108.7
343.15	0.1	1011.0	1036.7	1068.6	1103.2
353.15	0.1	1004.8	1029.2	1062.6	1096.3
363.15	0.1	997.0	1023.2	1055.7	1088.8
373.15	0.7	990.5	1016.2	1049.4	1082.4
383.15	0.7	983.1	1009.2	1043.9	1076.6
393.15	0.7	975.7	1002.3	1036.7	1069.9
403.15	0.7	967.8	994.6	1029.8	1063.1
413.15	0.7	960.5	987.6	1023.3	1057.5

[a] w_2 is the mass fraction of MEA in the (water + MEA) solutions. [b] The uncertainties are given in Table 12.

dx.doi.org/10.1021/je2010038 | J. Chem. Eng. Data 2012, 57, 1095–1103

Table 6. Liquid Densities ρ for Water (1) + MEA (2) + CO_2 (3) from T = (298.15 to 413.15) K and CO_2 Loading from α = (0.10 to 0.47) n_{CO_2}/n_{MEA} at w_2 = 0.5[a,b]

		α			
T/K	p/MPa	0.10	0.22	0.34	0.47
		ρ/kg·m^{-3}			
298.15	0.1	1054.4	1090.5	1130.8	1166.8
313.15	0.1	1044.8	1081.7	1122.5	1158.5
323.15	0.1	1038.4	1075.7	1116.8	1152.8
333.15	0.1	1032.0	1069.7	1110.8	1146.9
343.15	0.1	1025.2	1063.2	1104.8	1140.8
353.15	0.1	1018.3	1056.7	1098.5	1134.5
363.15	0.1	1011.0	1049.9	1092.0	1127.3
373.15	0.7	1004.5	1043.0	1085.4	1119.6
383.15	0.7	997.5	1036.9	1079.7	1112.5
393.15	0.7	990.8	1028.8	1073.9	1104.8
403.15	0.7	983.3	1021.0	1067.9	1098.4
413.15	0.7	976.8	1012.8	1061.2	1092.6

[a] w_2 is the mass fraction of MEA in the (water + MEA) solutions. [b] The uncertainties are given in Table 12.

Table 7. Liquid Densities ρ for Water (1) + MEA (2) + CO_2 (3) from T = (298.15 to 413.15) K and CO_2 Loading from α = (0.10 to 0.48) n_{CO_2}/n_{MEA} at w_2 = 0.6[a,b]

		α			
T/K	p/MPa	0.10	0.22	0.34	0.48
		ρ/kg·m^{-3}			
298.15	0.1	1065.3	1099.3	1153.6	1200.2
313.15	0.1	1055.4	1088.9	1145.0	1191.6
323.15	0.1	1048.9	1081.7	1139.1	1185.8
333.15	0.1	1042.1	1074.4	1133.1	1179.8
343.15	0.1	1035.1	1066.6	1127.0	1173.7
353.15	0.1	1028.0	1058.0	1120.7	1167.8
363.15	0.1	1020.6	1049.4	1114.3	1160.6
373.15	0.7	1014.5	1042.3	1107.0	1153.7
383.15	0.7	1007.3	1035.3	1098.3	1147.8
393.15	0.7	1000.7	1028.9	1092.2	1141.3
403.15	0.7	994.9	1022.3	1085.7	1136.3
413.15	0.7	989.6	1017.1	1079.5	1130.4

[a] w_2 is the mass fraction of MEA in the (water + MEA) solutions. [b] The uncertainties are given in Table 12.

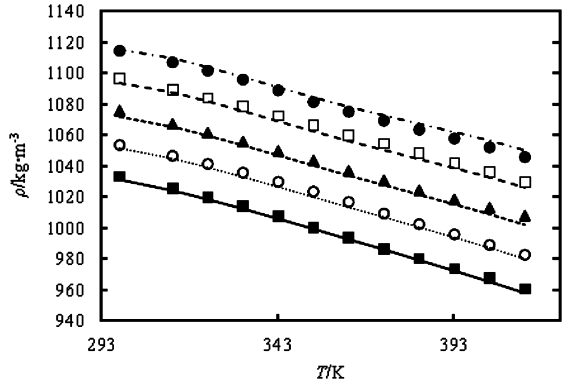

Figure 4. Densities of H_2O (1) + MEA (2) + CO_2 (3) solutions as a function of temperature at mass fraction of MEA = 0.3 and different CO_2 loadings. Symbols refer to experimental data: ■, α = 0.10; ○, α = 0.21; ▲, α = 0.32; □, α = 0.44; ●, α = 0.56. Lines are correlated data: —, α = 0.10; ···, α = 0.21; ---, α = 0.32; ——, α = 0.44; -·-, α = 0.56.

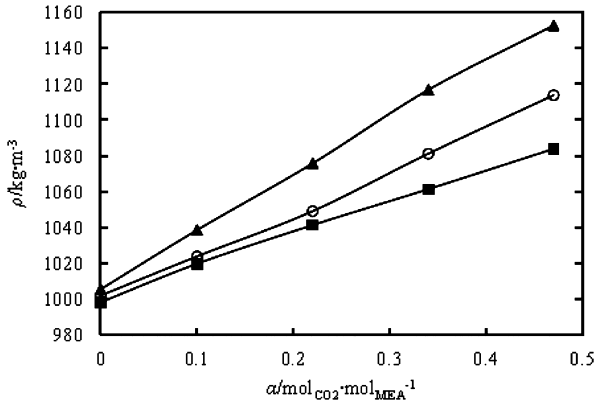

Figure 5. Densities of H_2O (1) + MEA (2) + CO_2 (3) solutions as a function of CO_2 loading at 323.15 K and different mass fractions of MEA: ■, 0.3; ○, 0.4; ▲, 0.5.

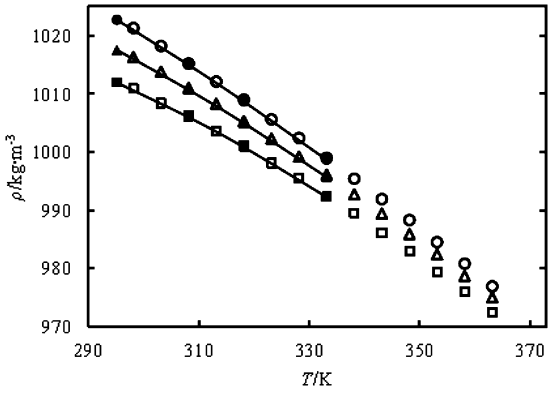

Figure 6. Comparison of measured and literature densities of H_2O (1) + MEA (2) solutions for three mass fractions of MEA. This work □, 0.3; △, 0.4; ○, 0.5; and values from Pouryousefi and Idem.[13] ■, 0.3; ▲, 0.4; ●, 0.5.

Surface tensions of aqueous MEA solutions are tabulated in Table 8. The surface tension varies with temperatures and concentrations as shown in Figure 8. It was observed that as the temperature increases the surface tension of aqueous MEA solutions decreases. This is because when the temperature increases, thermal motion of molecules increases, molecules at the surface stretch more, intermolecular attraction decreases, and then the surface tension decreases. It can be also seen from Figure 8 that the surface tension decreases as mass fraction of MEA increases. Measured surface tensions of aqueous MEA solutions are compared with the data from Vázquez et al.[15] at 303.15 K in Figure 9. The maximum deviation between them is 0.0048 N·m^{-1}.

■ MODEL FOR DATA REPRESENTATION

Densities of unloaded aqueous MEA solutions from this work have been analyzed by calculating the excess molar volumes. These are in turn correlated by the Redlich–Kister[17] equation with parameters being fitted by nonlinear regression analysis. The excess molar volumes are defined by

$$V_m^E/m^3\cdot mol^{-1} = V_m/m^3\cdot mol^{-1} - ((V_1^o/m^3\cdot mol^{-1})x_1 + (V_2^o/m^3\cdot mol^{-1})x_2) \quad (1)$$

where V_m represents the molar volume of the mixture. Furthermore V_j and x_j are the molar volume and mole fraction

dx.doi.org/10.1021/je2010038 | J. Chem. Eng. Data 2012, 57, 1095–1103

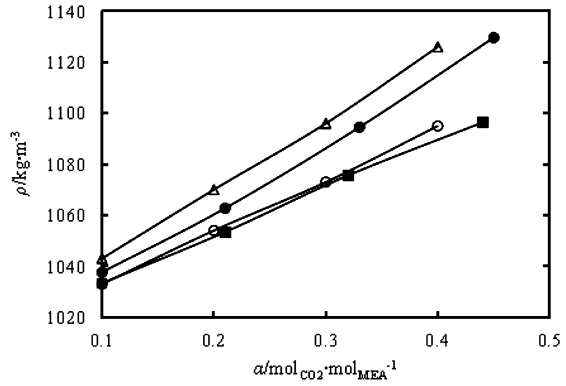

Figure 7. Densities of H_2O (1) + MEA (2) + CO_2 (3) solutions as a function for CO_2 loading at 298.15 K and different mass fractions of MEA. Results from this work: ■, w_2 = 0.3; ● w_2 = 0.4; are compared to results from Weiland et al.:[11] ○, w_2 = 0.3; △, w_2 = 0.4.

Table 8. Surface Tension γ for Water (1) + MEA (2) from T = (303.15 to 333.15) K and Mass Fraction of MEA from 0 to 1.0[a]

		T/K			
w_2	x_2	303.15	313.15	323.15	333.15
		γ/N·m^{-1}			
0	0	0.0713	0.0696	0.0680	0.0662
0.1	0.032	0.0668	0.0655	0.0643	0.0625
0.2	0.069	0.0647	0.0633	0.0617	0.0601
0.3	0.112	0.0636	0.0626	0.0612	0.0594
0.4	0.164	0.0617	0.0603	0.0588	0.0573
0.5	0.228	0.0593	0.0582	0.0569	0.0554
0.6	0.307	0.0574	0.0564	0.0552	0.0536
0.7	0.407	0.0558	0.0548	0.0534	0.0518
0.8	0.541	0.0534	0.0524	0.0511	0.0496
0.9	0.726	0.0506	0.0496	0.0484	0.0470
1.0	1	0.0481	0.0467	0.0456	0.0446

[a]The uncertainties are given in Table 12.

respectively for component j. j = 1 refers to water, and 2 to MEA. The superscript o refers to the pure component data.

The excess molar volumes are correlated with the polynomial equation from Redlich−Kister by least-squares fitting of the parameters A_i.

$$V_m^E/\mathrm{m^3\cdot mol^{-1}} = x_2(1-x_2)\sum_{i=0}^{i=n} A_i(1-2x_2)^i\cdot 10^{-6} \quad (2)$$

Here A_i are adjustable parameters, and the n represents an integer varying from 1 to how big a number can be justified by the data. The excess volumes derived from the density data and used as basis for the correlation work are tabulated in Table 3.

It was decided to use a third-order form of eq 3, that is, i was varied from 0 to 3. The fourth parameter reduces the average relative deviation (ARD) by roughly 75 %. The parameters of the Redlich−Kister equation may in turn be fitted to an empirical function of temperature as suggested by Mandal et al.[12] In their case a second-order polynomial in temperature was used. As in their work the parameters and their temperature relationship was regressed in one go using nonlinear regression

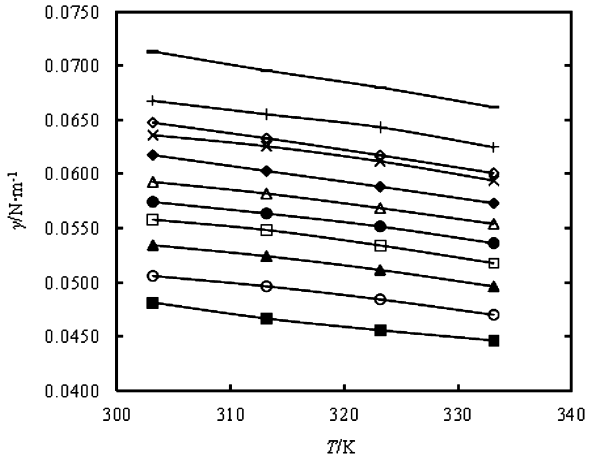

Figure 8. Surface tensions of H_2O (1) + MEA (2) solutions as a function of temperature at different mass fractions of MEA: ■, MEA; ○, 0.9; ▲, 0.8; □, 0.7; ●, 0.6; △, 0.5; ♦, 0.4; ×, 0.3; ◊, 0.2; +, 0.1; —, water.

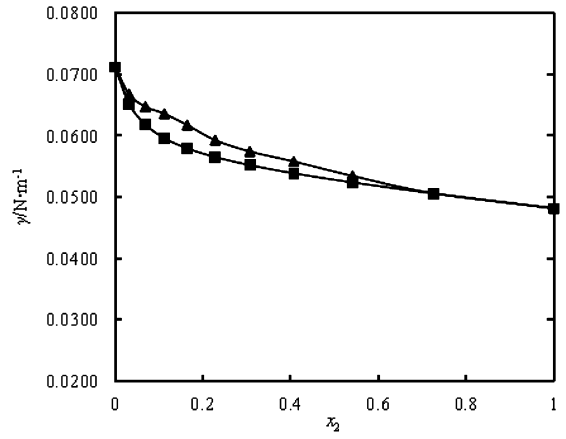

Figure 9. Comparison with literature of the H_2O (1) + MEA (2) surface tension data as a function of mole fraction at 303.15 K. ▲, our results; ■, results from Vázquez et al.[15]

analysis. However, in this work it was found that a linear temperature relationship of the type

$$A_i = a_{i0} + a_{i1}(T/\mathrm{K} - 273.15) \quad (3)$$

for all of the Redlich−Kister parameters represented our data well. The a_{ij}'s are the linear parameters for each A_i and T is the temperature. The regression data were inspected, and no systematic error related to temperature was seen. The coefficients A_i for fitting the Redlich−Kister eq 4 to excess molar volumes for binary aqueous MEA solutions from (298.15 to 423.15) K are presented in Table 9.

The correlation for the excess volumes is defined by eqs 2 and 3 and Table 9. Using this to correlate solution densities, the average absolute deviation (AAD) for densities is 0.83 kg·m^{-3}, and the maximum deviation is 2.9 kg·m^{-3}. These errors are negligible for engineering estimates.

A correlation for estimating the density of CO_2-loaded aqueous amine solution is available in a recent publication.[11] Molar volumes have been calculated by eq 4 to analyze

dx.doi.org/10.1021/je2010038 | J. Chem. Eng. Data 2012, 57, 1095−1103

Table 9. Coefficients Fitted to Equations 2 and 3 by Nonlinear Regression Analysis

Redlich−Kister parameter	R-K temperature coefficient	values derived
A_0	a_{00}	−2.643
	a_{01}	0.00260
A_1	a_{10}	−0.690
	a_{11}	0.00189
A_2	a_{20}	0.440
	a_{21}	−0.0000318
A_3	a_{30}	1.870
	a_{31}	−0.00123

densities of CO_2-loaded aqueous MEA solutions. The correlated model is described by eqs 5 and 6.

$$V/\mathrm{m^3{\cdot}mol^{-1}} = [x_1(M_1/\mathrm{kg{\cdot}mol^{-1}}) + x_2(M_2/\mathrm{kg{\cdot}mol^{-1}}) + x_3(M_3/\mathrm{kg{\cdot}mol^{-1}})]/(\rho/\mathrm{kg{\cdot}m^{-3}}) \quad (4)$$

$$V/\mathrm{m^3{\cdot}mol^{-1}} = x_1(V_1/\mathrm{m^3{\cdot}mol^{-1}}) + x_2(V_2/\mathrm{m^3{\cdot}mol^{-1}}) + (x_3V_{\mathrm{CO_2}} + x_1x_2V^{*} + x_2x_3V^{**})\cdot 10^{-6} \quad (5)$$

$$V^{**} = c + dx_2 \quad (6)$$

Here V_j, x_j, M_j, and ρ_j are mole volume, mole fraction, molar mass, and density, respectively, for component j. No subscript refers to the mixture, j = 1 refers to water, 2 to MEA, and 3 to CO_2. V_1 and V_2 are calculated by the values from Table 3. V_{CO_2}, V^*, c, and d are free parameters which are attained by nonlinear regression analysis with two independent variables. The parameters are in turn fitted to the polynomial function of temperature.

$$V_{\mathrm{CO_2}} = a_0 + a_1(T/\mathrm{K} - 273.15) + a_2(T/\mathrm{K} - 273.15)^2 + a_3(T/\mathrm{K} - 273.15)^3 + a_4(T/\mathrm{K} - 273.15)^4 \quad (7)$$

$$V^{*} = b_0 + b_1(T/\mathrm{K} - 273.15) + b_2(T/\mathrm{K} - 273.15)^2 + b_3(T/\mathrm{K} - 273.15)^3 \quad (8)$$

$$c = c_0 + c_1(T/\mathrm{K} - 273.15) + c_2(T/\mathrm{K} - 273.15)^2 + c_3(T/\mathrm{K} - 273.15)^3 \quad (9)$$

$$d = d_0 + d_1(T/\mathrm{K} - 273.15) + d_2(T/\mathrm{K} - 273.15)^2 + d_3(T/\mathrm{K} - 273.15)^3 \quad (10)$$

The values of the fitted coefficients in eqs 7 to 10 are presented in Table 10. The average absolute deviation between the correlation results and our experimental data is 3.8 $\mathrm{kg{\cdot}m^{-3}}$, and the maximum deviation is 16 $\mathrm{kg{\cdot}m^{-3}}$. The agreement between the correlated and the experimental densities is satisfactory.

The surface tensions of binary mixtures were correlated with temperature by a linear relationship.

$$\gamma_{\mathrm{mix}}/\mathrm{N{\cdot}m^{-1}} = K_1 - K_2(T/\mathrm{K} - 273.15) \quad (11)$$

The parameters K_1 and K_2 are listed in Table 11. The average absolute deviation is 0.0001 $\mathrm{N{\cdot}m^{-1}}$, and the maximum deviation is 0.0002 $\mathrm{N{\cdot}m^{-1}}$. The correlated surface tensions by

Table 10. Parameters for Liquid Density Correlations of CO_2-Loaded MEA Solutions

parameters		values derived
V_{CO_2}	a_0	12.6520
	a_1	−0.4065
	a_2	0.0096
	a_3	−0.000077
	a_4	0.00000017
V^*	b_0	−2.6676
	b_1	0.0016
	b_2	0.00013
	b_3	−0.0000015
c	c_0	−25.3952
	c_1	1.2716
	c_2	−0.03845
	c_3	0.00023
d	d_0	73.6487
	d_1	−3.9579
	d_2	0.1029
	d_3	−0.00059

eq 11 and the experimental data have good agreement. The deviations are within experimental error.

The surface tensions of mixtures were correlated with the mole fraction by the chemical model of Connors and Wright.[18]

$$\gamma_{\mathrm{mix}}/\mathrm{N{\cdot}m^{-1}} = \gamma_1/\mathrm{N{\cdot}m^{-1}} + \sum_{j\geq 2}\left(1 + \frac{a_ix_i}{(1-b_i)\left(1 + \sum_{j\geq 2}\frac{b_i}{(1-b_i)}x_i\right)}\right) \times x_j((\gamma_j/\mathrm{N{\cdot}m^{-1}}) - (\gamma_1/\mathrm{N{\cdot}m^{-1}})) \quad (12)$$

This model includes two adjustable parameters, a_2 and b_2, for a system with two components. The fitted values of a_2 and b_2 are also presented in Table 11. The average absolute deviation is 0.0004 $\mathrm{N{\cdot}m^{-1}}$ and the maximum deviation is 0.0013 $\mathrm{N{\cdot}m^{-1}}$. These deviations are larger than the results correlated by eq 11, but still acceptable.

■ ASSESSMENT OF THE EXPERIMENTAL UNCERTAINTIES

The uncertainty of density measurements of unloaded aqueous MEA solutions arises from several sources involved in the temperature rise measurement, the error from mass fraction of MEA, and instrument error. For the DMA 4500 the temperature accuracy is specified as ± 0.03 K. Based on our measurement results, the change of density is 0.8 $\mathrm{kg{\cdot}m^{-3}}$ when the change of temperature is 1 K. So this leads to an uncertainty in ρ of 0.024 $\mathrm{kg{\cdot}m^{-3}}$. For the DMA HP the temperature accuracy is specified as ± 0.05 K. This leads to an uncertainty in ρ of 0.04 $\mathrm{kg{\cdot}m^{-3}}$. The accuracy of mass fraction of MEA is estimated as ± 0.005. The maximum change of density is 6.6 $\mathrm{kg{\cdot}m^{-3}}$ when the change of mass fraction is 0.1. This corresponds to an uncertainty in ρ of 0.33 $\mathrm{kg{\cdot}m^{-3}}$. The instrument accuracy for DMA 4500 used at T < 373.15 K is given as 0.05 $\mathrm{kg{\cdot}m^{-3}}$ by the manufacturer, while for DMA HP used at $T \geq$ 373.15 K is given as 0.1 $\mathrm{kg{\cdot}m^{-3}}$. The uncertainty

dx.doi.org/10.1021/je2010038 | J. Chem. Eng. Data 2012, 57, 1095−1103

Table 11. Surface Tension Parameters for Water (1) + MEA (2) Solutions

x_2	K_1	K_2	x_2	K_1	K_2	T/K	a_2	b_2
0.000	0.07639	0.0001699	0.307	0.06132	0.0001263	303.15	0.5127	0.8964
0.032	0.07109	0.0001407	0.407	0.05999	0.0001345	313.15	0.4632	0.9017
0.069	0.06947	0.0001558	0.541	0.05737	0.0001270	323.15	0.4754	0.8942
0.112	0.06795	0.0001396	0.726	0.05430	0.0001198	333.15	0.5106	0.8827
0.164	0.06619	0.0001480	1.000	0.05146	0.0001158			
0.228	0.06327	0.0001298						

in ρ is determined as 0.34 kg·m^{-3} at T < 373.15 K and 0.35 kg·m^{-3} at $T \geq$ 373.15 K by combining the various sources of uncertainty using a root-sum-of-squares formula. The combined expanded uncertainty of density of unloaded aqueous MEA solutions is $U_c(\rho)$ = 0.68 kg·m^{-3} at T < 373.15 K and $U_c(\rho)$ = 0.70 kg·m^{-3} at $T \geq$ 373.15 K (level of confidence = 0.95).

Similar to the previous calculations, the uncertainty of density measurements of CO_2-loaded aqueous MEA solutions arises from several sources involved in the temperature rise measurement, the error from mass fraction of MEA, the error from CO_2 loading amount, and instrument error. The uncertainty in ρ is determined as 1.3 kg·m^{-3} for the whole temperature range by combining the various sources of uncertainty. The combined expanded uncertainty of the density of CO_2-loaded aqueous MEA solutions is $U_c(\rho)$ = 2.6 kg·m^{-3} (level of confidence = 0.95).

The uncertainty of surface tension measurements of aqueous MEA solutions is determined as 0.0002 N·m^{-1} by combining the error from temperature measurement, mass fraction of MEA, and instrument error. The combined expanded uncertainty of surface tension of aqueous MEA solutions is $U_c(\gamma)$ = 0.0004 N·m^{-1} (level of confidence = 0.95). The uncertainties of the original measurements and the resulting combined uncertainties are shown in Table 12.

Table 12. Uncertainties of the Density and Surface Tension Measurements

density measurements		surface tension measurements	
$u(T)$	0.03 K at T < 373.15 K 0.05 K at $T \geq$ 373.15 K	$u(T)$	0.2 K
$u(w_2)$	0.005	$u(w_2)$	0.005
instrument accuracy	0.05 kg·m^{-3} at T < 373.15 K 0.1 kg·m^{-3} at $T \geq$ 373.15 K	instrument accuracy[19]	0.00003 N·m^{-1}
$u(\alpha)$	0.003 mol_{CO_2}·mol_{MEA}^{-1}		
$U_c(\rho)$ of unloaded MEA solutions	0.68 kg·m^{-3} at T < 373.15 K	$U_c(\gamma)$ of unloaded MEA solutions	0.0004 N·m^{-1}
$U_c(\rho)$ of CO_2-loaded MEA solutions	0.70 kg·m^{-3} at $T \geq$ 373.15 K 2.6 kg·m^{-3}		

The uncertainty that caused by the error from mass fraction of MEA dominates in the uncertainties of unloaded aqueous MEA solutions density and surface tension measurements. Moreover, the uncertainty from the CO_2 loading amount dominates the uncertainties of CO_2-loaded aqueous MEA solution density measurements.

CONCLUSIONS

Densities in the H_2O (1) + MEA (2) mixtures have been measured in the temperature range between (298.15 and 423.15) K for mass fractions of MEA from 0.3 to 1.0. The data are correlated using excess molar volumes to represent the deviations from ideal mixtures. The errors in the values of the densities predicted using the Redlich−Kister equation with fitted parameters to represent excess molar volumes are on average 0.83 kg·m^{-3}.

Densities of CO_2-loaded aqueous MEA solutions have been measured at temperatures from (298.15 to 413.15) K with the mass fraction of MEA of 0.3, 0.4, 0.5, and 0.6. Densities of CO_2-loaded aqueous MEA solutions decrease with temperature and increase with CO_2 loading. Densities of CO_2-loaded solutions are higher than unloaded solutions. Not unexpectedly, the densities increase faster with CO_2 loading when the concentration of MEA is higher. The equations from Weiland et al.[11] were used to correlate the density data. The AAD between the correlated and the experimental densities is 3.8 kg·m^{-3}.

Surface tensions in H_2O (1) + MEA (2) mixtures have been measured at temperatures from (303.15 to 333.15) K. The concentration range was from 0 to 1.0. As the temperature increased, the surface tension of aqueous MEA solutions decreased. Moreover, the surface tension of aqueous MEA solutions decreased as the mole fraction of MEA increased for a given temperature. The surface tension data were correlated with temperature and mole fraction. The AADs between the correlated and the experimental surface tensions are 0.0001 N·m^{-1} and 0.0004 N·m^{-1}, respectively.

The models fitted to the density and surface tension data constitute a satisfactory representation with errors that would be negligible for engineering estimates.

AUTHOR INFORMATION

Corresponding Author

*E-mail: morten.c.melaaen@hit.no. Telephone number: +47 35575286. Fax number: +47 35575001.

Funding

The authors would like to thank the Norwegian Research Council and Statoil for financial support.

Notes

The authors declare no competing financial interest.

ACKNOWLEDGMENTS

The assistance of Mishan Rai, Trond Risberg, and Sigbjørn Wiersdalen is gratefully acknowledged.

REFERENCES

(1) Leibush, A. G.; Shorina, E. G. Physico-Chemical Properties of Ethanolamine. *Zh. Prikl. Khim.* **1947**, *20*, 69−76.

(2) Touhara, H.; Okazaki, S.; Okino, F.; Tanaka, H.; Ikari, K.; Nakanishi, K. Thermodynamic properties of aqueous mixtures of hydrophilic compounds 2. Aminoethanol and its methyl derivatives. *J. Chem. Thermodyn.* **1982**, *14*, 145−156.

(3) Murrieta-Guevara, F.; Rodriguez, A. T. Liquid Density as a Function of Temperature of Five Organic Solvents. *J. Chem. Eng. Data* **1984**, *29*, 204−206.

(4) Wang, Y. W.; Xu, S.; Otto, F. D.; Mather, A. E. Solubility of N_2O in alkanolamines and in mixed solvents. *Chem. Eng. J.* **1992**, *48*, 31−40.
(5) Li, M. H.; Shen, K. P. Densities and Solubilities of Solutions of Carbon Dioxide in Water + Monoethanolamine + *N*-Methyldiethanolamine. *J. Chem. Eng. Data* **1992**, *37*, 288−290.
(6) DiGullio, R. M.; Lee, R. J.; Schaeffer, S. T.; Brasher, L. L.; Teja, A. S. Densities and Viscosities of the Ethanolamines. *J. Chem. Eng. Data* **1992**, *37*, 239−242.
(7) Pagé, M.; Huot, J.; Jolicoeur, C. A comprehensive thermodynamic investigation of water-ethanolamine mixtures at 10, 25, and 40 °C. *Can. J. Chem.* **1993**, *71*, 1064−1072.
(8) Maham, Y.; Teng, T. T.; Hepler, L. G.; Mather, A. E. Densities, Excess Molar Volumes, and Partial Molar Volumes for Binary Mixtures of Water with Monoethanolamine, Diethanolamine, and Triethanolamine from 25 to 80 °C. *J. Solution Chem.* **1994**, *23*, 195−205.
(9) Li, M.; Lie, Y. Densities and Viscosities of Solutions Monoethanolamine + N-Methyldiethanolamine + Water and Monoethanolamine + 2-Amino-2-methyl-1-propanol + Water. *J. Chem. Eng. Data* **1994**, *39*, 444−447.
(10) Lee, M.; Lin, T. Density and Viscosity for Monoethanolamine + Water, + Ethanol, and + 2-Propanol. *J. Chem. Eng. Data* **1995**, *40*, 336−339.
(11) Weiland, R. H.; Dingman, J. C.; Cronin, D. B.; Browning, G. J. Density and Viscosity of Some Partially Carbonated Aqueous Alkanolamine Solutions and Their Blends. *J. Chem. Eng. Data* **1998**, *43*, 378−382.
(12) Mandal, B. P.; Kundu, M.; Bandyopadhyay, S. S. Density and Viscosity of Aqueous Solutions of (N-Methyldiethanolamine + Monoethanolamine), (N-Methyldiethanolamine + Diethanolamine), (2-Amino-2-methyl-1-propanol + Monoethanolamine), (2-Amino-2-methyl-1-propanol + Diethanolamine). *J. Chem. Eng. Data* **2003**, *48*, 703−707.
(13) Pouryosefi, F.; Idem, R. O. New Analytical Technique for Carbon Dioxide Absorption Solvents. *Ind. Eng. Chem. Res.* **2008**, *47*, 1268−1276.
(14) Amundsen, T. G.; Øi, L. E.; Eimer, D. A. Density and Viscosity of Monoethanolamine + Water + Carbon Dioxide from (25 to 80) °C. *J. Chem. Eng. Data* **2009**, *54*, 3096−3100.
(15) Vázquez, G.; Alvarez, E.; Navaza, J. M.; Rendo, R.; Romero, E. Surface Tension of Binary Mixtures of Water + Monoethanolamine and Water + 2-Amino-2-methyl-1-propanol and Tertiary Mixtures of These Amines with Water from 25 to 50 °C. *J. Chem. Eng. Data* **1997**, *42*, 57−59.
(16) Harvey, A. H. *Thermodynamic Properties of Water*; NIST: Boulder, CO, 1998.
(17) Redlich, O.; Kister, A. T. Algebraic representation of thermodynamic properties and the classification of solutions. *Ind. Eng. Chem.* **1948**, *40*, 345−348.
(18) Connors, K. A.; Wright, J. L. Dependence of Surface Tension on Composition of Binary Aqueous-Organic Solutions. *Anal. Chem.* **1989**, *61*, 194−198.
(19) Hansen, F. K. Surface Tension by Image Analysis: Fast and Automatic Measurements of Pendant and Sessile Drops and Bubbles. *J. Colloid Interface Sci.* **1993**, *160*, 209−217.